DOI 10.1007/s11182-017-1150-3

Russian Physics Journal, Vol. 60, No. 5, September, 2017 (Russian Original No. 5, May, 2017)

PHOTOLUMINESCENCE CHARACTERISTICS OF YAG:Ce, Gd BASED PHOSPHORS WITH DIFFERENT PREHISTORIES

V. M. Lisitsyn,[1] N. P. Soshchin,[2] Yu Yang yang,[1] S. A. Stepanov,[1] L. A. Lisitsyna,[3] A. T. Tulegenova,[1,4] and Kh. A. Abdullin[4]

UDC 535.37

Luminescence characteristics of yttrium-aluminum garnet based phosphor samples differed by their elemental composition and prehistory of synthesis are studied. The morphology, structure, and elemental composition of phosphor samples, their excitation and emission spectra, efficiency of phosphor conversion of chip emission, and kinetics of luminescence decay are measured. The emission characteristics of phosphors are compared with their structural properties and elemental composition.

Keywords: yttrium aluminum garnet, structure, elemental composition, luminescence, kinetics, spectra, efficiency.

INTRODUCTION

Phosphors based on yttrium-aluminum garnet (YAG) $Y_3Al_5O_{12}$ are perspective materials for conversion of UV and blue emission of light-emitting diodes (LEDs) by InGaN based chips into emission in the visible range of the spectrum [1–4]. Excitation of the YAG phosphor doped by trivalent cerium in the region 340 or 460 nm leads to the occurrence of intensive luminescence in the region 500–650 nm. A modification of phosphors through incorporation of modifiers can be used to displace the position of the emission band in the spectrum [5]. The use of the chip emitting at 460 nm for phosphor excitation seems most promising. This chip has minimal excitation energy losses for phosphor conversion of the emission into the visible range, and the efficiency of energy conversion can reach 0.76 [6]. Integral emission of such light-emitting diode is the sum of the phosphor emission and the blue chip emission partly transmitted through the composite with phosphor. By the present time great progress has been made in improving technologies of synthesis of effective YAG phosphors for white LEDs. Further increase in the conversion efficiency is impossible without understanding of elementary processes providing high degree of emission conversion and their relationship with the structure, elementary composition, and imperfection of synthesized phosphors.

The present work studies the dependence of the emission characteristics of YAG phosphors of SDL type on their initial structural characteristics.

[1]National Research Tomsk Polytechnic University, Tomsk, Russia, e-mail: lisitsyn@tpu.ru; 1374586947@qq.com; stepanovsa@tpu.ru; [2]Federal State Unitary Enterprise Scientific-Research Institute "PLATAN," Moscow Region, Fryazino, Russia, e-mail: soschin@mail.ru; [3]Tomsk University of Architecture and Building, Tomsk, Russia, e-mail: lisitsyna@mail.ru; [4]Al-Farabi Kazakh National University, Ministry of Education and Science of the Republic of Kazakhstan, Almaty, the Republic of Kazakhstan, e-mail: tulegenova.aida@gmail.com; kh.a.abdullin@mail.ru. Translated from Izvestiya Vysshikh Uchebnykh Zavedenii, Fizika, No. 5, pp. 106–112, May, 2017. Original article submitted January 26, 2017.

TABLE 1. Elemental Composition of the Examined Samples

Phosphor	Y	Al	O	Gd	Ce
SDL2700-2016	9.55	5.06	53.22	20.98	11.21
SDL2700-2015	8.62	4.21	56.98	20.86	9.32
SDL3500-2015	25.13	4.54	49.00	4.09	17.24
SDL3500-2016	26.07	4.28	55.32	4.41	9.92
SDL4000-2016	35.51	4.73	59.77		
SDL4000-2015	36.57	5.16	58.27		

1. EXAMINED SAMPLES AND EXPERIMENTAL TECHNIQUE

We studied industrial SDL4000 ($Y_3Al_5O_{12}$), SDL3500 ($Y_{2.6}Gd_{0.25}Al_5O_{12}:Ce_{0,15}$), and SDL2700 ($Y_{1.24}Gd_{1.56}Al_5O_{12}:Ce_{0.2}$) phosphors synthesized in the Research and Production Association "PLATAN" in 2015 and 2016. The elemental composition of the synthesized samples was studied using an x-ray photoelectron spectrometer (XPS) ESCALAB 250 with a PHI 5000Versaprobe-Scanning ESC Amicroprobe. The elemental composition of the examined samples is presented in Table 1. Phosphors SDL2700 and SDL3500 contain Gd and Ce in addition to Y, Al, and O. Phosphors SDL4000 had no Gd and Ce in quantities, sufficient for detection by the employed method. We emphasize that the method employed allowed the sample composition to be determined only near its surface. The morphology of phosphors was studied with a scanning electron microscope (SEM) Quanta3D 200i. The structure of phosphors was identified using an x-ray diffractometer (XRD) Rigaku with CuK_α emission. The photoluminescence spectra were recorded using a spectrometer FLS980 with a xenon lamp (250–1000 nm) as an excitation source. The ultraviolet semiconductor laser (λ_{em} = 375 nm and τ = 0.75 ns) was used as an excitation source for measuring the decay kinetics.

2. EXPERIMENTAL RESULTS

2.1. Crystal structure

As an example, Fig. 1 shows SEM images of SDL4000 phosphor samples synthesized in different years. The following differences can be indicated in the morphology of phosphor particles. All SDL4000 phosphors consist of particles whose maximal sizes do not exceed 20 μm. Many particles of SDL2700 phosphor have sizes greater than 20 μm, and particles of SDL3500 are about 20 μm. The large particles are contained in the most part of volumes of SDL2700 and SDL3500 phosphors, and they are contained in a smaller part of the volume of SDL4000 phosphor. Small particles have micron and submicron sizes. Attention is attracted to the following. Particles of SDL4000-2015 phosphor are shaped as pure granules bounded by planes. Granules of the SDL4000-2016 phosphor are more rounded and covered by spiderweb that does not penetrate into the particles.

Many particles incompletely formed into crystals and small particles of submicron sizes are characteristic for SDL3500-2015 phosphors. These particles are more smooth, without faceting characteristic for crystals. Particles of SDL2700 phosphors are shaped as granules with a tendency toward faceting. All large particles are covered by small particles resembling fragments with sizes fluctuating from 200 nm to several micrometers. We note that sizes and shapes of phosphor particles are similar to those reported in [7].

Figure 2 shows x-ray diffraction patterns of the examined phosphors. For a comparison, the x-ray diffraction pattern of the YAG crystal is shown. All diffraction peaks correspond to the YAG phase. Some changes revealed in the relationships of the peak intensities are probably because of the incorporation of Ce^{3+} and Gd^{3+} ions. It is established that the position of the (420) diffraction peak in phosphors is shifted toward smaller angles relative to that in the crystal. It is suggested that the displacement of the (420) peak is caused by the distortion of the lattice due to the substitution of

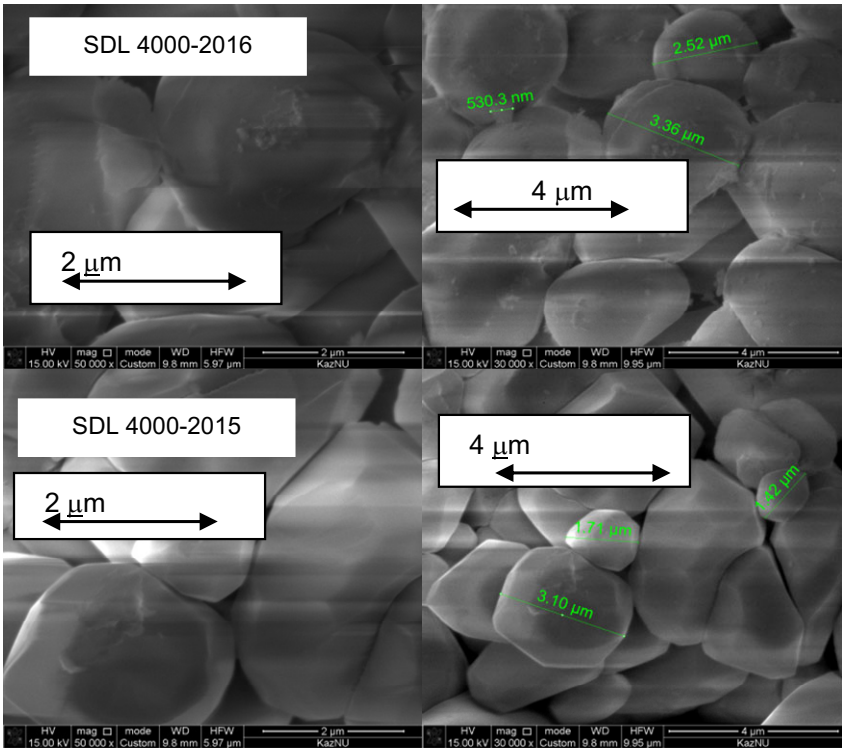

Fig. 1. Example of SEM images of SDL4000 samples synthesized in 2016 and 2015.

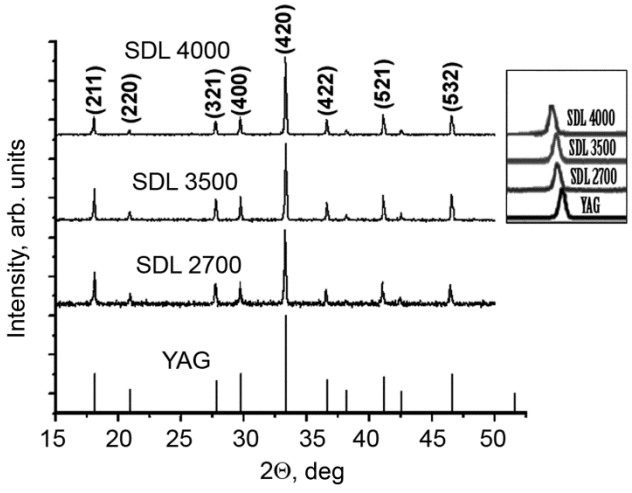

Fig. 2. X-ray diffraction patterns of SDL4000, SDL3500, and SDL2700 $Y_3Al_5O_{12}$ crystals. Positions of the (420) peaks for the examined samples are shown in the inset.

Y^{3+} (0.92 Å) ions by Gd^{3+} (0.938 Å) ions. The recorded x-ray diffraction patterns are analogous to those measured in [7, 8].

TABLE 2. Characteristics of the Emission and Excitation Spectra of Examined Phosphors: Position of the Band Maximum and Its Halfwidth

Phosphor	Characteristics of excitation bands				Characteristics of the excitation bands in the luminescence band maxima			
	λ_{ex} = 460 nm		λ_{ex} = 340 nm		In the region 340 nm		In the region 460 nm	
	ΔE, eV	λ_{max}, nm	ΔE, eV	λ_{max}, nm	ΔE, eV	λ_{max}, nm	ΔE, eV	λ_{max}, nm
SDL2700-2015	0.487	585 ± 2	0.489	580 ± 2	0.264	336 ± 2	0.450	460 ± 2
SDL2700-2016	0.487	583 ± 2	0.489	580 ± 2	0.273	336 ± 2	0.468	460 ± 2
SDL3500-2015	0.484	562 ± 2	0.487	558 ± 2	0.294	338 ± 2	0.390	458 ± 2
SDL3500-2016	0.484	560 ± 2	0.487	558 ± 2	0.304	338 ± 2	0.411	458 ± 2
SDL4000-2015	0.435	540 ± 2	0.486	540 ± 2	0.313	340 ± 2	0.396	456 ± 2
SDL4000-2016	0.447	545 ± 2	0.504	545 ± 2	0.324	340 ± 2	0.426	456 ± 2

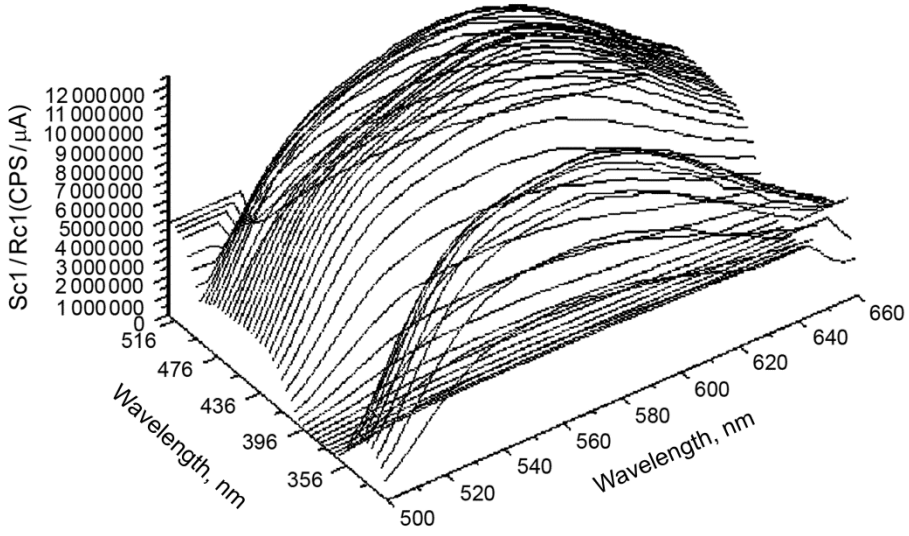

Fig. 3. Excitation and luminescence spectra of SDL4000-2015 phosphors.

2.2. Luminescence and excitation spectra

The luminescence and excitation spectra were measured at wavelengths in the range 300–510 nm. An example of the measured luminescence and excitation spectra in the 3D format is shown in Fig. 3. Two peaks at 339 and 456 nm can be distinguished in the excitation spectrum. The excitation peak at 456 nm coincides well with the absorption band of YAG phosphors and crystals [9–11] and the blue emission band of the InGaN based chip. Therefore, YAG phosphors effectively absorb chip emission and convert it into longer-wave one.

The spectral characteristics of phosphors in generalized form, including positions of luminescence and excitation bands and their halfwidths, are presented in Table 2. The positions of the luminescence bands are independent of the spectral range in which the luminescence was excited. The measured excitation and luminescence spectra are analogous to the spectra measured for YAG phosphors [12] and crystals [13, 14].

The following regularities were established for the results presented above. The luminescence band of SDL4000 phosphor in the region 454 nm (~0.44 eV) was narrower than the bands of SDL2700 and SDL3500 phosphors

TABLE 3. Luminescence Energy Yield η under 460 nm Excitation and Characteristic Times of Luminescence Decay in the Band Maxima under 375 nm Excitation

Serial No.	Phosphors	τ_1, ns	A_1, rel.%	τ_2, ns	A_2, rel.%	τ, ns	η
1	SDL2700-2015	4.2	10.4	66.1	89.6	59.6	0.422
2	SDL2700-2016	4.3	14.9	66.0	85.1	56.8	0.393
3	SDL3500-2015	1.5	12.3	60.5	87.7	53.4	0.438
4	SDL3500-2016	4.0	9.7	68.7	90.3	62.4	0.368
5	SDL4000-2015	3.0	12.7	61.8	87.3	54.4	0.377
6	SDL4000-2016	2.9	9.1	59.8	90.9	54.6	0.404

(~0.485 eV). The luminescence band of SDL4000 phosphor in the region 344 nm (~0.495 eV) was wider than that in the region 454 nm (~0.44 eV). The halfwidths of the excitation band in the region 340 nm differed for all examined phosphors and changed from 0.264 to 0.324 eV. The excitation band widths in the region 460 nm differed for all examined phosphors and changed from 0.390 to 0.450 eV.

2.3. Efficiency of phosphor conversion of chip emission

The integral efficiency of phosphor conversion of chip emission was measured using an integrating sphere and an AvaSpec-ULS3648 calibrated spectrometer. The energy yield of the emission conversion η was measured as a ratio of the flux emitted by phosphor to the absorbed excitation flux. For excitation, the chip generating emission with a flux of 173 μW/cm^2 in the band at 460 nm in the plane of phosphor arrangement was used. The measured η values are presented in Table 3.

2.4. Kinetics of luminescence decay

Curves of phosphor luminescence decay were investigated. As an excitation source, a pulsed light-emitting diode of the EPLED series emitting a 750 ps pulse at 375 nm with bandwidth of about 10 nm was used. As an example, Fig. 4 shows the kinetics of SDL3500-2015 luminescence decay in the band maximum.

Kinetic curves of luminescence decay in all phosphors in the nanosecond range had a clearly expressed two-stage character. They were fairly well described by the function

$$I = A_1 \exp(-t / \tau_1) + A_2 \exp(-t / \tau_2),$$

where A_1 and A_2 are the initial intensities, and τ_1 and τ_2 are the characteristic luminescence decay times. Results of investigation of the kinetic of luminescence decay curves are summarized in Table 3. The short-term decay component in the nanosecond range for the examined phosphors was within 1.46–4.3 ns, and the long-term component was within 59.8–68.7 ns. The main portion of the entire emission was provided by the long-term component: 87.3–90.9%. The average decay time τ was 53–59 ns. This is in agreement with the data presented in [13, 15, 16].

2.5. Dispersion of decay times

For all examined phosphors, the dependences of the kinetic curves on the wavelength of the recorded luminescence were measured in the nanosecond range. The characteristic decay times were calculated from the results of measurements, and the dependences of these times on the wavelengths (the dispersion of the characteristic times) were drawn.

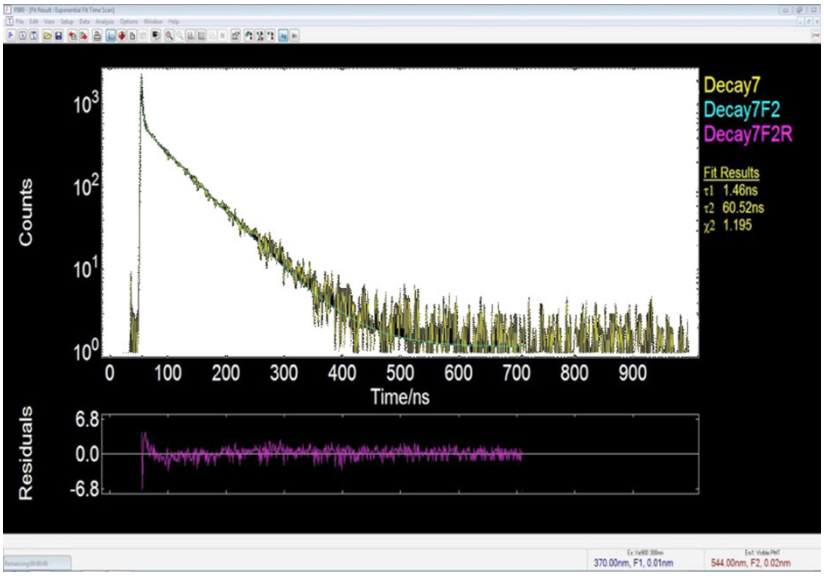

Fig. 4. Kinetics of luminescence decay of SDL3500-2015 phosphor.

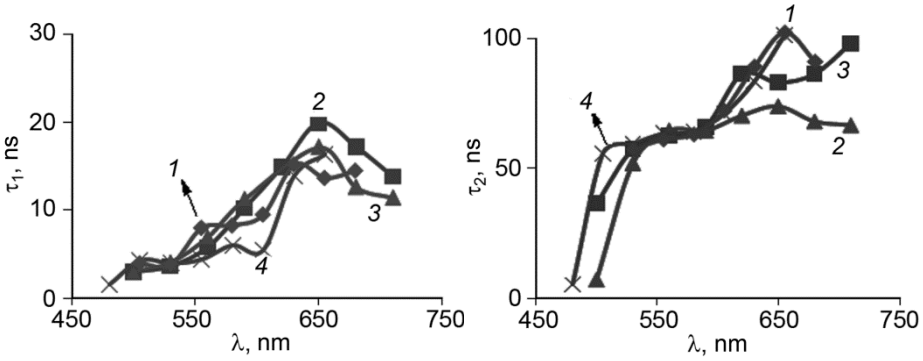

Fig. 5. Dispersion of the luminescence decay times.

The results of measurements are shown in Fig. 5 for short- and long-term components. Two segments are distinguished in the dispersion curves. At wavelengths from 480 to 610 nm, the characteristic times were shorter than in the long-wave region of the spectrum. This means that the luminescence centers in these regions of the spectrum have different characteristics. We note that the sharp decrease of the decay time at wavelengths less than 480 nm demonstrates that the dominant emission in this region was the emission of the chip rather than of phosphor.

3. DISCUSSION OF RESULTS

Our studies of phosphors have shown that they are very imperfect and contain considerable number of not only intentionally incorporated activators and modifiers, but also intrinsic defects of the lattice. In the SEM images, the particles do not shaped as well faceted crystals. Among the phosphor particles, smoother, obviously incompletely formed crystals are often encountered. The results of XRD analysis demonstrated that the main characteristics of the x-ray diffraction patters were similar to those of crystals, but the difference in the relationships of the peak intensities for phosphors of one type but synthesized in different years were obvious. The lattice parameter changed when yttrium is substituted by gadolinium. The results of our investigations demonstrated that the elemental compositions of phosphors

of one type synthesized in different years differed considerably. Hence, even at strict adherence to technological conditions of synthesis, the materials obtained had different degrees of imperfection.

This conclusion seems reasonable: it is impossible to provide high degree of stoichiometry when crystals are synthesized from the mixture of three-four components. Moreover, in such complicated compounds as YAG phosphors, the existence of antidefects (mutual substitution of cations) is possible. It is obvious that disorders created in the crystal during synthesis should be compensated by incorporation of intrinsic structural defects – vacancies and interstitial ions. And finally, in a very imperfect crystal such as phosphor, the defects cannot be distributed homogeneously throughout the volume. Complexes consisting of structural elements and defects of the lattice having nanometer sizes are formed in the crystal. Their existence was confirmed for LiF based scintillation crystals with polyvalent impurity [17] and for $ZnWO_4$ [18]. Nanodefects are effective centers for trapping excitation energy and its transfer to the luminescence centers being structural elements of the nanodefect structure.

Results of investigation of the emission characteristics of phosphors allowed us to conclude the following. The integral efficiency of energy conversion of chip emission into luminescence in all examined phosphors was high and equal to 48–58% of its limiting value [6]. The luminescence excitation spectra were absolutely similar. This testifies to the similarity of the excitation processes. Hence, the excitation processes are independent of changes in the elemental composition and the degree of imperfection of phosphors of this group. The luminescence spectra of phosphors of different types differed. This testifies to different luminescence centers or their combination and is confirmed by the investigation of the dispersion of the decay times. We note that the long-term components with τ of about 2 and 20 μs that contribute significantly to the integral luminescence were observed for all examined phosphors [19].

This suggests that the luminescence in YAG phosphors is caused by excitation and relaxation of Ce^{3+} ions. In [20, 21] it was shown that the cerium centers can have different surroundings, and a portion of luminescence can be caused by the *F*-centers. We believe that in very imperfect YAG phosphors, as in oxygen-containing scintillation crystals, the luminescence centers are complex defects whose structure involves oxygen-vacancy complexes [17, 18].

The authors express their gratitude to Y. Wang, Professor of Jilin University, for kindly provided possibility of carrying out spectral and structural measurements.

REFERENCES

1. N. P. Soshchin, N. A. Gal'china, L. M. Kogan, *et al*., Fiz. Tekh. Poluprovodn., **43**, No. 5, 700–704 (2009).
2. A. V. Aladov, E. D. Vasil'eva, A. L. Zakgeim, *et al*., Svetotekhnika, No. 3, 8–16 (2010).
3. K. Li and C. Shen, Optik, No. 123, 621–623 (2012).
4. N. A. Gal'china, A. L. Gofshtein-Gardt, L. M. Kogan, and N. P. Soshchin, Svetotekhnika, No. 4, 51–53 (2010).
5. Ch. M. Briskina, S. I. Rumyantsev, M. V. Ryzhkov, *et al*., Svetotekhnika, No. 5, 37–39 (2012).
6. V. M. Lisitsyn, S. A. Stepanov, Y. Yu, and V. S. Lukash, AIP Conf. Proc., **1698**, 060008-1–060008-5 (2016).
7. W. Jun, H. Tao, L. Tianchun, *et al*., Int. J. Electrochem. Sci., No. 10, 2554 – 2563 (2015).
8. S. Hongling, Z. Chen, H. Jiquan, *et al*., Opt. Mater. Express, **4**, No. 4, 649–655 (2014).
9. D. Yongjun, Z. Guoqing, X. Jun, *et al*., J. Crystal Growth, No. 286, 476–480 (2006).
10. D. Yongjun, Z. Guoqing, X. Jun, *et al*., Mater. Res. Bull., No. 41, 1959–1963 (2006).
11. S. Nishiura, S. Tanabe, K. Fujioka, and Y. Fujimoto, Opt. Mater., No. 33, 688–691 (2011).
12. S. Qinglin, Z. Zhiwei, X. Changtai, *et al*., Opt. Mater., No. 35, 2155–2159 (2013).
13. Y. Xinbo, L. Hongjun, B. Qunyu, *et al*., J. Crystal Growth, **311**, 3692–3696 (2009).
14. V. M. Lisitsyn, Kh. A. Abdullin, S. A. Stepanov, *et al*., Izv. Vyssh. Uchebn. Zaved. Fiz., **59**, No. 9/2, 164–168 (2016).
15. D. T. Valiev, S. A. Stepanov, EW. A. Vishnyakova, *et al*., Izv. Vyssh. Uchebn. Zaved. Fiz., **58**, No. 6/2, 42–47 (2015).
16. V. M. Lisitsyn, S. A. Stepanov, V. A. Vaganov, and A. T. Tulegenova, Izv. Vyssh. Uchebn. Zavrd. Fiz., **59**, No. 9/2, 169–173 (2016).
17. L. A. Lisitsyna and V. M. Lisitsyn, Phys. Solid State, **55**, No. 11, 2297–2303 (2013).

18. V. M. Lisitsyn, D. T. Valiev, I. A. Tupitsyna, *et al*., J. Lumin., **153**, 130–135 (2014).
19. V. M. Lisitsyn, S. A. Stepanov, D. T. Valiev, *et al*., IOP Conf. Series: Mater. Sci. Eng., **110**, 012051-1–012051-5 (2016).
20. G. R. Asatryan, D. D. Kramushchenko, Yu. A. Uspenskaya, *et al*., Fiz. Tverd. Tela, **56**, No. 6, 1106–1111 (2014).
21. V. V. Seminko, P. O. Maksimchuk, N. V. Kononets, *et al*., Visnik KhNU. Fiz., **26**, 20–23 (2016).